Platelet Endothelial Cell Adhesion Molecule 1 (PECAM-1) and Its Interactions with Glycosaminoglycans: 2. Biochemical Analyses[†]

Deirdre R. Coombe,*[,‡] Sandra M. Stevenson,[‡] Beverley F. Kinnear,[‡] Neha S. Gandhi,[‡] Ricardo L. Mancera,[‡,§] Ronald I. W. Osmond,[‡,||] and Warren C. Kett[‡]

School of Biomedical Sciences and Western Australian Biomedical Research Institute, and School of Pharmacy, Curtin University of Technology, GPO Box U1987, Perth, Western Australia 6845, Australia

Received December 17, 2007; Revised Manuscript Received February 11, 2008

ABSTRACT: Platelet endothelial cell adhesion molecule 1 (PECAM-1) (CD31), a member of the immunoglobulin (Ig) superfamily of cell adhesion molecules with six Ig-like domains, has a range of functions, notably its contributions to leukocyte extravasation during inflammation and in maintaining vascular endothelial integrity. Although PECAM-1 is known to mediate cell adhesion by homophilic binding via domain 1, a number of PECAM-1 heterophilic ligands have been proposed. Here, the possibility that heparin and heparan sulfate (HS) are ligands for PECAM-1 was reinvestigated. The extracellular domain of PECAM-1 was expressed first as a fusion protein with the Fc region of human IgG1 fused to domain 6 and second with an N-terminal Flag tag on domain 1 (Flag-PECAM-1). Both proteins bound heparin immobilized on a biosensor chip in surface plasmon resonance (SPR) binding experiments. Binding was pH-sensitive but is easily measured at slightly acidic pH. A series of PECAM-1 domain deletions, prepared in both expression systems, were tested for heparin binding. This revealed that the main heparin-binding site required both domains 2 and 3. Flag-PECAM-1 and a Flag protein containing domains 1–3 bound HS on melanoma cell surfaces, but a Flag protein containing domains 1–2 did not. Heparin oligosaccharides inhibited Flag-PECAM-1 from binding immobilized heparin, with certain structures having greater inhibitory activity than others. Molecular modeling similarly identified the junction of domains 2 and 3 as the heparin-binding site and further revealed the importance of the iduronic acid conformation for binding. PECAM-1 does bind heparin/HS but by a site that is distinct from that required for homophilic binding.

Platelet endothelial cell adhesion molecule 1 (PECAM-1)[1] (CD31) is a member of the cell adhesion molecule subgroup of the immunoglobulin (Ig) superfamily of glycoproteins. It is a heavily glycosylated protein of approximately 130 kDa of the following structure: an extracellular domain comprising six C2-type Ig domains, followed by a short single transmembrane domain and a cytoplasmic tail of 118 amino acids (*1, 2*). Its expression is confined to cells of the vascular system, more particularly to endothelial cells, monocytes, neutrophils, platelets, a subpopulation of circulating T-lymphocytes (primarily CD8+, CD45RA naïve lymphocytes), and CD43+ hemopoietic progenitor cells in the bone marrow. The cytoplasmic tail is coded by eight exons, which undergo alternative splicing to produce splice variants that are expressed in a developmentally and tissue-specific manner (*3*). Although the cytoplasmic tail does not possess any catalytic activity, PECAM-1 mediates signal transduction via the interactions of its tail with a series of adaptor proteins. Central to many of these interactions are two tyrosine residues, Y663 and Y686, each of which fall within an immunoreceptor tyrosine inhibitory motif (ITIM). Phosphorylation of these two residues creates sites for the binding and activation of signaling molecules containing Src homology (SH2) domains (*4*). This association with various cytosolic molecules contributes to the regulation of the cellular localization and functions of PECAM-1.

PECAM-1 has a wide range of functions. Experimental evidence from both *in vitro* and *in vivo* studies indicates that PECAM-1 plays a role in the extravasation of monocytes and neutrophils at sites of inflammation (*1, 5*). Initial studies

[†] This study was supported in part by a grant to D.R.C. from Meditech Research Ltd., Melbourne, Australia, and by a Curtin University Internal Grant to N.S.G.

* To whom correspondence should be addressed: Molecular Immunology, School of Biomedical Sciences, Curtin University of Technology, Level 5 MRF Building, Rear 50 Murray Street, Perth, Western Australia 6845, Australia. Telephone: +61-8-9224-0355. Fax: +61-8-9224-0360. E-mail: d.coombe@curtin.edu.au.

[‡] School of Biomedical Sciences and Western Australian Biomedical Research Institute.

[§] School of Pharmacy.

[||] Present address: TGR BioSciences Pty Ltd., P.O. Box 185, Hindmarsh, South Australia 5007, Australia.

[1] Abbreviations: PECAM-1, platelet endothelial cell adhesion molecule 1; HS, heparan sulfate; Ig, immunoglobulin; ITIM, immunoreceptor tyrosine inhibitory motif; GAG, glycosaminoglycan; mAb, monoclonal antibody; DP, degree of polymerization; IdoA, α-L-iduronic acid; GlcA, β-D-glucuronic acid; GlcA2S, 2-*O*-sulfated glucuronic acid; IdoA2S, 2-*O*-sulfated iduronic acid; GlcN, D-glucosamine; GlcNS6S, *N*-sulfo-D-glucosamine-6-*O*-sulfate; PDB, Protein Data Bank; SPR, surface plasmon resonance; HAB, heparin−albumin−biotin; MALDI−MS, matrix-assisted laser desorption/ionization time-of-flight mass spectrometry; VEGF, vascular endothelial growth factor; GM-CSF, granulocyte-macrophage colony-stimulating factor; rmsd, root-mean-square deviation; FGF-2, basic fibroblast derived growth factor; streptavidin–HRP, horseradish-peroxidase-conjugated streptavidin; SAX, strong anion exchange.

10.1021/bi7024595 CCC: $40.75
Published on Web 03/08/2008

using blocking anti-PECAM-1 antibodies suggested a role in angiogenesis, and this conclusion has been supported by the observation of reduced angiogenesis in mice deficient in PECAM-1 expression (*4*). Other studies have described PECAM-1 as potently suppressing apoptosis in a number of cell systems (*6*). PECAM-1 has also been implicated in hemostasis through its inhibitory effects on platelet aggregation and spreading and thrombosis formation (*7*). However, these conclusions have recently been questioned (*8*). PECAM-1 is required for normal megakaryocytokinesis because it plays an essential role in the migration of megakaryocytes within the bone marrow stroma, and in PECAM-1-deficient mice recovery of the peripheral platelet count is impaired following induced thrombocytopenia (*9*). Interestingly, PECAM-1 is a marker of cells capable of early hemopoietic potential in the human embryo (*10*). To understand the contribution of PECAM-1 to normal physiological processes and to disease, it is essential to also understand what ligands are involved in PECAM-1-mediated adhesion and signaling to determine the range of cellular targets with which PECAM-1 positive cells interact.

The interactions of PECAM-1 with its ligands are complex. It is accepted that PECAM-1 mediates cell−cell adhesion by binding PECAM-1 on adjacent cells (homophilic binding). These trans homophilic interactions also trigger intracellular signaling via the ITIM domains, and such signaling events are important for many of the functional activities of PECAM-1. The first Ig domain is critically important for trans homophilic interactions (*11*). A number of heterophilic ligands have also been described for PECAM-1. These include the integrin, $\alpha_v\beta_3$ (*12*), CD38, which is widely expressed on cell surfaces (*13*), glycosaminoglycans (GAGs) of the heparin/heparan sulfate family (*14, 15*), and more recently the neutrophil-specific glycoprotein CD177 (*16*). The likelihood that PECAM-1 binds directly to $\alpha_v\beta_3$ has been questioned (*17*), as well as the suggestion that heparan sulfate (HS) acts as a PECAM-1 ligand (*18*).

Some years ago, we published that PECAM-1 binds HS (*15*). A number of publications from other groups supported our findings. Indeed, it was believed that heparin bound to domain 2 of PECAM-1, because peptides mimicking an apparent GAG-binding consensus sequence inhibited activities attributed to PECAM-1−GAG binding events (*14, 19*). A similar amino acid motif was identified in the Ig superfamily neuronal cell adhesion molecule (NCAM), which has been shown to bind HS. Other papers suggested that alternative splicing of the cytoplasmic domain determined whether PECAM-1 bound in a homo- or heterophilic fashion to HS (*20, 21*). In these studies, the assays used to assess PECAM-1-binding behavior were cell-based and complex, and it was possible that other cell-surface molecules were contributing to the reactions seen.

Another publication concluded that cell-surface GAGs are not ligands for PECAM-1 (*18*). Here, it was argued that heparin affects PECAM-1 adhesion by indirect mechanisms that are downstream of the engagement of PECAM-1 with its ligands. Moreover, it was claimed that PECAM-1/IgG chimeric proteins bound heparin because they included an engineered amino acid sequence in the hinge region that conferred GAG-binding properties that were not normally present. In this study, we have reinvestigated PECAM-1−heparin/HS binding and now report that the extracellular domain of PECAM-1 does bind heparin and HS in biochemical experiments; it also binds HS on cell surfaces. Binding is pH-sensitive, and stable binding occurs at a pH that allows the protonation of histidines. Two expression systems were used to express the extracellular domains of PECAM-1, and both produced comparable data. Moreover, domain-deletion experiments revealed that the heparin/HS-binding regions of PECAM-1 are distinct from those involved in homophilic binding.

MATERIALS AND METHODS

Materials. Chondroitin sulfate A from bovine trachea, chondroitin sulfate B (dermatan sulfate) from porcine skin, and chondroitin sulfate C from shark cartilage were from Sigma (St. Louis, MO). Heparin and HS from porcine mucosa was obtained from Celsus Laboratories (Cincinnati, OH). Heparinase I, EC 4.2.2.7, was obtained from Grampian Enzymes (Harray, Orkney, Scotland), and heparinase III, EC 4.2.2.8, was from Ibex Technologies, Inc. (Montreal, Canada). The mouse anti-HS monoclonal antibody (mAb), HepSS-1, was obtained from Seikagaku Corporation (Tokyo, Japan). The anti-PECAM-1 polyclonal IgG antibody (sheep) was obtained from R&D Systems, Inc. (Minneapolis, MN). The anti-PECAM-1 polyclonal antibody (rabbit) was a generous gift from Dr. Michael Berndt (then of the Baker Medical Research Institute, Melbourne, Australia). The biotin-conjugated anti-sheep Ig was from Zymed Laboratories (San Francisco, CA). The control IgM antibody was from Serotec Ltd. (Kidlington, Oxford, U.K.), and the FITC-conjugated anti-mouse Ig and the FITC-conjugated anti-rabbit were from Dako-Cytomation (Golstrup, Denmark).

Cell Culture. COS-7 cells (ECACC, Porton Down, U.K.) were grown in RPMI/10% FCS and cultured using standard methods, but immediately before transfection, the media was replaced with RPMI/1% FCS depleted of immunoglobulin by affinity chromatography on protein A Sepharose (Pharmacia Corp., Skokie, IL). The human melanoma cell line A2058 from the European Collection of Animal Cell Cultures (ECACC) was maintained as described (*22*). Sulfated GAG-deficient cells were prepared by culturing A2058 cells in sulfate-free minimum Eagle's medium (MEM, Sigma-Aldrich, St Louis, MO) and 25 mM $NaClO_3$ for 48 h essentially as described (*22*) but with the modification of culturing the cells for 18 h in MEM medium with no sulfate prior to the addition of 97.7 mg/L $MgSO_4$ (control) or $NaClO_3$. Cells for flow cytometry were harvested using phosphate-buffered saline (PBS) containing 2.5 mM ethylenediaminetetraacetic acid (EDTA), washed, and resuspended in 10 mM Bis-Tris (pH 6.3) containing 150 mM NaCl and 0.5% BSA (Bis-Tris/BSA) or PBS containing 0.5% BSA.

Construction and Purification of PECAM-1-Fc Chimeric Fusion Proteins. These constructs were a kind gift from Dr. David Simmons (then of the Institute of Molecular Medicine, Oxford, U.K.) and are described in detail elsewhere (*23*). Briefly, the constructs were comprised of cDNA of the various extracellular Ig domains of PECAM-1 fused to the Fc portion of human IgG1. Constructs of a nested series of domain deletions were produced as follows, all of which contained NH_2-terminal domain 1: domain 1-Fc (D1-Fc), domains 1–2-Fc (D1–2-Fc), domains 1–3-Fc (D1–3-Fc), domains 1–4-Fc (D1–4-Fc), domains 1–5-Fc (D1–5-Fc),

Table 1: Primers Used for PCR

Description	Sequence
5'end PECAM-1 (nt 58-78) introducing *HinDIII* site	5'-CTGCTCTGTTCAAAGCTTATG$_{78}$ *HinDIII*
3' end PECAM-1 domain 2 (nt 684-711) introducing "stop" codon.	5'-CTTGGGTGTCTAGAAGGATTCCGTCACG$_{684}$
3'end PECAM-1 domain 3 (nt 970-995) introducing "stop" codon.	5'-GATTCCAGTTCGGGCTAGGAAAATAG$_{970}$
3' end PECAM-1 domain 6 (nt 1793 to introduced "stop")	5'-GGGCTATGTTTTCTTCCATG$_{1793}$
3' end PECAM-1 domain 1 (nt 363-390) introducing *Eco R1* site	5'-CATGAATTCCTTCCACCAACAGCTGGTACTC$_{363}$ *EcoR1*
5' end PECAM-1 domain 3 (nt 707-733) inc. *Eco R1* site	5'-ATGAATTCCCAAGTTCCACATCAGCCCCACCGGA$_{733}$ *EcoR1*
5' end PECAM-1 domain 4 (nt 982-1005) inc. *Eco R1* site	5'-ATGAATTCCCGAACTGGAATCTTCCTTCACA$_{1005}$ *EcoR1*
5' end PECAM-1 domain 5 (nt 1231-1258) inc. *EcoR1* site	5'-ATGAATTCCCAGGATTTCTTATGATGCCCAGTTTG$_{1258}$ *EcoR1*
5' end PECAM-1 domain 6 (nt 1495-1518) inc. *EcoR1* site	5'-ATGAATTCCGGTGGATGAGGTCCAGATTTCT$_{1518}$ *EcoR1*

and domains 1–6-Fc (D1–6-Fc). These were cloned into pCDM8 vector (Invitrogen, Carlsbad, CA) for expression in COS-7 cells. The hinge region of these constructs was sequenced and found to consist of the amino acids, P W K K > T E < P K S C D K T H T C, which corresponds to the four COOH-terminal amino acids of PECAM-1 D6 > hinge < human IgG1 C_H2 domain. The PECAM-1-Fc fusion plasmids were electroporated into COS-7 cells and allowed to express for ~72 h. Cell supernatants containing the secreted proteins were harvested, filtered, and affinity-purified using protein A Sepharose and standard methods. Proteins were concentrated, aliquoted, and stored at −20 °C. Sizes of all expressed proteins were confirmed by appropriate gel electrophoresis.

Construction and Purification of Flag-PECAM-1 Proteins. pFlag-CMV1 vector (Sigma-Aldrich) is designed to express proteins with a preprotrypsin leader sequence fused to a NH_2-terminal Flag octapeptide (DYKDDDDK) for affinity purification. The human PECAM-1 cDNA 5′ end was modified by the polymerase chain reaction (PCR) to remove the native PECAM-1 leader sequence and introduce a *Hin*D III restriction site. cDNAs for domains 1–2, 1–3, and 1–6 were produced by PCR and subcloned into pGEM-T (Promega Corp., Madison, WI) vector. These were digested from pGEM with *Hin*D III and *Spe* I and cloned into *Hin*D III and *Xba* I sites of pFlag. A NH_2-terminal domain 1 (D1) construct incorporating a 3′-end *Eco*R I site was also cloned into pFlag. This was then used to make fusion constructs: D1 fused to domain 3 (D1 plus D3), D1 fused to domains 3–6 (D1 plus D3–6), D1 fused to domains 4–6 (D1 plus D4–6), D1 fused to domains 5–6 (D1 plus D5–6), and D1 fused to domain 6 (D1 plus D6) (Figure 4A).

The PCR strategy for obtaining these constructs was as follows: PCR conditions were ~50 ng template, 1 μM primers, 2.5 mM $MgCl_2$, 150 μM dNTP mix, and 1 unit of Taq polymerase per reaction. Cycles: denaturation at 92 °C for 30 s, annealing at 63 °C first 3 cycles, then at 68 °C for a subsequent 37 cycles for 60 s, and elongation at 74 °C for 60 s. The primers used are given in Table 1. All PCR products were ligated into pGEM-T, then removed with the appropriate restriction enzymes, and cloned into the pFlag-domain 1 construct. All constructs were sequenced and found to correspond to the published sequence. DNA was electroporated into COS-7 cells and allowed to express for ~72 h. Supernatants were then harvested, filtered, and purified using an anti-Flag agarose affinity column (Sigma-Aldrich) and standard methods. Proteins were concentrated, aliquoted, and stored at −20 °C. Sizes of all PCR products and expressed proteins were confirmed by appropriate gel electrophoresis.

Surface Plasmon Resonance (SPR) Analyses. SPR analyses were performed on BIAcore 2000 (BIAcore AB, Uppsala, Sweden). One flow cell of a streptavidin sensor chip (BIAcore, Melbourne, Australia) was derivatized with heparin (Celsus Laboratories, Cincinnati, OH) that had been biotinylated at the reducing terminus, as previously described (*24*). An increase of between 200 and 400 resonance units, depending upon the experiment, indicated heparin had been immobilized. A second flow cell was saturated with biotin for use as a control surface. PECAM-1 proteins were dissolved in 10 mM Bis-Tris, 150 mM NaCl, 0.005% Tween-20, and 2 mM EDTA, which was adjusted to the designated pH (usually 6.3) and injected over the heparinized and control surfaces at a flow rate of 30 μL/min. After a 2.5 min dissociation, the sensor surface was regenerated with 30 μL of 2 M NaCl. The response was monitored as a function of time at 25 °C. For GAG or heparin oligosaccharide inhibition experiments, Flag-PECAM-1 was mixed with the various oligosaccharide preparations prior to injection over the biosensor surface. Binding sensorgrams were obtained by subtracting the response of control flow cells.

PECAM-1−Heparin Enzyme-Linked Immunosorbent Assay (ELISA). Microtiter plates (Nunc Maxisorp, Roskilde, Denmark) were coated by incubation with Anti-FLAG (M2) mAb (Sigma-Aldrich) in 100 mM $NaHCO_3$ at pH 8.4 overnight at 4 °C. Plates were then blocked in PBS, 0.05% Tween 20, and 1% BSA (PBST/BSA). Flag-PECAM-1 proteins in PBST/BSA were serially diluted across the plate (starting concentration of 80 nM) and incubated 1 h at 37 °C. Heparin−albumin−biotin (Sigma-Aldrich) at 50 μL (0.625 μg in 10 mM Bis-Tris at pH 6.3, 150 mM NaCl, 0.05% Tween 20, and 1% BSA) was added to the wells, incubated for 1 h at 37 °C and then washed with the same buffer. Detection was by streptavidin−horseradish peroxidase (HRP)

(Amersham Biosciences, Piscataway, NJ) in the Bis-Tris buffer. After incubation for 1 h at 37 °C, TMB substrate (KPL, Gaithersburg, MD) was applied, color was developed for 30 min at room temperature and then stopped by the addition of 1 M H_3PO_4, and the plate was read at an absorbance of 405 nM using a Wallac Victor 1420 Plate Reader (Wallac, Turku, Finland). Controls were M2 mAb, heparin−albumin−biotin, and streptavidin−HRP.

Flow Cytometry. A2058 cells were stained for HS using the HepSS-1 mAb as described, except that 10×10^4 cells per test were used (*22*). Cells (10×10^4) were incubated with Flag-PECAM-1(D1–6) or its truncations, Flag-(D1–2) or Flag-(D1–3), at a concentration of 4.2 μg/test for 1 h at room temperature in Bis-Tris/BSA (10 mM Bis-Tris at pH 6.3, 150 mM NaCl, and 1% BSA). Binding of the PECAM-1 proteins was visualized using an anti-PECAM-1 polyclonal antibody (sheep), followed by biotin-conjugated anti-sheep IgG, and streptavidin−Alexa 488. For inhibition experiments, Flag-PECAM-1 or Flag-(D1–3) were mixed with HS or chondroitin sulfate C (1–50 μg/test), incubated for 1 h at room temperature, before adding to the cells and incubating for 1 h at room temperature, and then stained as described. Sulfated GAG-depleted cells were incubated with Flag-PECAM-1 and stained using the rabbit anti-PECAM-1 polyclonal antibody followed by FITC-conjugated anti-rabbit antibody. For heparinase III treatment, 10×10^4 cells were incubated with 1 mIU heparinase III in RPMI/0.5% BSA for 30 min at 37 °C before being washed with Bis-Tris/BSA, incubated with Flag-PECAM-1, and then stained for chlorate-treated cells. Appropriate controls were included. The intensity of fluorescence was determined using a Coulter EPICS XL flow cytometer (Coulter Electronics, High Wycombe, U.K.).

Preparation of Heparin and HS Oligosaccharides. The enzymes heparinase I and III cleave at specific sites on the heparin/HS chain: heparinase I at IdoA residues with N-sulfated GlcN domains and heparinase III at GlcA residues in unsulfated *N*-acetyl GlcN domains.

Heparin and HS were depolymerized in accordance with the procedure described by Chai et al. (*25*). Briefly, heparin or HS (5 g) and albumin (4 mg) were dissolved in 50 mL of 30 mM CH_3CO_2Na containing 3 mM $CaCl_2$ and adjusted to pH 7 with 0.2 M $NaHCO_3$. Heparinase I (2 IU) or heparinase III (2 IU) was added, and the mixture was incubated at 30 °C for 16 h. The mixture was boiled for 3 min, aliquoted (5 mL), and frozen. Size-exclusion chromatography was performed on two 90 × 1.5 cm glass columns connected in series. The first column was packed with Bio-Gel P6 fine, and the second column was packed with Bio-Gel P10 fine (both from BioRad Laboratories, Inc., Hercules, CA). The columns were eluted with 0.25 M NaCl at a flow rate of 0.25 mL/min using a Gilson HPLC (Middleton, WI), and the effluent was monitored with a refractive index detector. Data were acquired using Gilson Unipoint software. Fractions (1 mL) adjacent to the peak maxima were pooled, lyophilized, and desalted on a fast desalting column (10 × 100 mm, Amersham Biosciences) to give pools of oligosaccharides of a uniform degree of polymerization (DP). The desalted fragments were lyophilized, redissolved in water, and stored at –20 °C. The concentration of each fragment was determined spectrophotometrically at 232 nm in 30 mM HCl using the extinction coefficient of 5500 mol^{-1} cm^{-1}. The size of the oligosaccharides were confirmed using matrix-assisted laser desorption/ionization time-of-flight mass spectrometry (MALDI−MS) as described (*26*).

Strong anion exchange (SAX)−high-performance liquid chromatography (HPLC) was performed on oligosaccharide pools of uniform size. A Gilson HPLC and a 250 × 4.5 mm Dionex (Sunnyvale, CA) Propac PA1 column were used and maintained at 40 °C. The column was eluted at 1.0 mL/min with a binary gradient formed from two buffers. Buffer A was 10 mM Na_2HPO_4 adjusted to pH 7.0. Buffer B was 10 mM Na_2HPO_4 plus 2 M NaCl adjusted to pH 7.0. The gradient was 10% initially for 3 min and increased linearly to 40% at 6 min, 70% at 75 min, and 100% at 76 min, where it was maintained for 4 min. The column was equilibrated for 7 min between injections. The effluent was monitored at 232 nm. Fractions were pooled from several injections, concentrated, and desalted prior to screening for Flag-PECAM-1 binding activity. To concentrate, fractions were diluted with water to decrease salt concentrations to below 0.4 M and passed over an anion-exchange cartridge (EconoQ, 5 mL, BioRad); after washing with 10 mL of water, the retained oligosaccharides were eluted with 3 column volumes of 2 M NaCl. The extracts from the cartridges were desalted using a fast desalting column.

Rechromatography was performed at pH 3 on the ProPac PA1 column. Buffer C was 10 mM H_3PO_4 adjusted to pH 3, and buffer D was 10 mM H_3PO_4 containing 2 M NaCl and adjusted to pH 3. The gradient was varied to suit each fraction. Fractions were desalted using the fast desalting column.

Molecular Modeling. Molecular modeling was performed using the homology model of PECAM-1 that was constructed in the preceding paper (*27*). The docking of heparin fragments was performed with AutoDock version 3.0 (*28*), using the protocol as described in the preceding paper (*27*), and the predicted free energies of binding were extracted. Heparin fragments of DP5 and DP6 with different conformations of their iduronic acid residues were modeled. The fragments modeled and the Protein Data Bank (PDB) codes of the protein structures from which they were extracted are given in Table 2. The hexasaccharide (referred to as construct 1) was built from the pentasaccharide (PDB code 2HYV) by taking the structure of monosaccharide units B−E and adding Glc*N*S6S(1 → 4)IdoA2S to the nonreducing terminus. The GlcNS6S was in the $^4C_1$ conformation, and IdoA2S was in the $^1C_4$ conformation. This disaccharide structure was extracted from the pentasaccharide, PDB code 2HYV, monosaccharide units B−C.

RESULTS

SPR Analysis of PECAM-1 Binding to Heparin. The six Ig-like extracellular domains of PECAM-1 were expressed as a Flag-tagged protein, with the Flag being placed on the N terminus. Flag-PECAM-1 was purified by affinity chromatography using an anti-Flag antibody column, and purity was checked using sodium dodecyl sulfate−polyacrylamide gel electrophoresis (SDS−PAGE) and silver staining. Various concentrations of Flag-PECAM-1, at pH 6.3, were passed over a biosensor chip, to which heparin molecules had been coupled via their reducing termini. It is clear from Figure 1A that Flag-PECAM-1 binds well to immobilized heparin

Table 2: Predicted Energies of Interaction of Heparin Oligosaccharides with Domains 2 and 3

Oligosaccharide[1]	PDB code	Intermolecular energy (kcal/mol)	Free energy of binding (kcal/mol)
IdoA2S – GlcNS6S – IdoA2S – GlcNS6S – IdoA2S[2] $^1C_4$ $^4C_1$ $^2S_0$ $^4C_1$ $^{2,5}B$	**1QQP**	-9.3	-0.9
IdoA2S[3] **– GlcNS6S – IdoA2S – GlcNS6S – IdoA2S**[2] $^1H_2$ $^4C_1$ $^1C_4$ $^4C_1$ $^1C_4$	**2HYV**	-19.7	-11.3
ΔUA2S – GlcNS6S – IdoA2S – GlcNS6S – IdoA2S – GlcNS6S[4] $^1H_2$ $^4C_1$ $^1C_4$ $^4C_1$ $^2S_0$ $^4C_1$	**1BFC**	+4.5	+15.0
ΔUA2S – GlcNS6S – IdoA2S - GlcNS6S – IdoA2S – GlcNS6S[4] $^1H_2$ $^4C_1$ $^1C_4$ $^4C_1$ $^2S_0$ $^4C_1$	**1XT3**	-14.7	-4.1
GlcNS6S – IdoA2S – GlcNS6S – IdoA2S – GlcNS6S – IdoA2S[5] $^4C_1$ $^1C_4$ $^4C_1$ $^1C_4$ $^4C_1$ $^1C_4$	**Construct 1** (2HYV)	-18.3	-7.7

[1] Oligosaccharides structures are shown with the ring conformations of the monosaccharide units given below. [2] Monosaccharide units are identified as A–E. [3] In the crystal structure, this residue is ΔUA2S. For modeling purposes, the double bond was removed but the $^1H_2$ conformation was retained. [4] Monosaccharide units are identified as A–F. [5] Monosaccharide units are identified as A′ and A–E. The structure B−E is identical to the tetrasaccharide, B−E, in the pentasaccharide extracted from 2HYV.

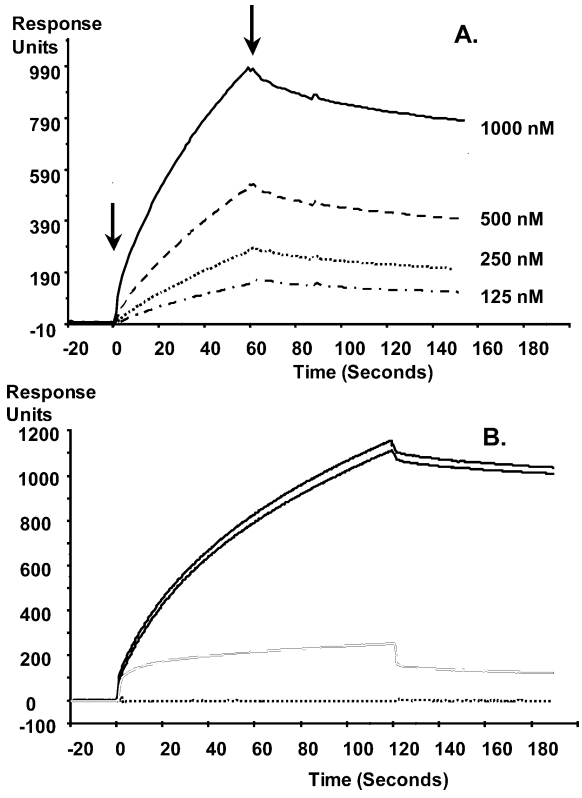

FIGURE 1: PECAM-1 extracellular domains bind heparin. (A) Various concentrations of Flag-PECAM-1 in a Bis-Tris saline buffer at pH 6.3 were passed over the heparin-coupled biosensor surface, and sensorgrams were generated. Arrows indicate the beginning and end of the protein injection. (B) Flag-PECAM-1 (1 μM) binding to immobilized heparin is blocked by HS. The protein is premixed with HS prior to injection. Bold black curves, Flag-PECAM-1 with no inhibitor; gray curve, Flag-PECAM-1 plus 2.5 μM HS; and dotted curve, negative control, Flag-PECAM-1 on the control surface with no immobilized heparin. Subtracted binding curves are shown. Different heparin-coupled biosensor chips were used for A and B.

under these conditions. Moreover, the binding of this PECAM-1 protein to immobilized heparin is blocked by HS when the protein is premixed with HS prior to injection over the biosensor surface. No binding of the HS containing buffer was detected (Figure 1B).

Some proteins have a pH optimum for binding GAGs that is not neutral, but because of the local conditions in the tissues, this is physiologically relevant and may serve to regulate the activity of the GAG-binding protein (*29*). Accordingly, the binding of Flag-PECAM-1 to immobilized heparin was examined using buffers of different pH, but the Flag-PECAM-1 sample tested and the heparin-coupled biosensor chip remained the same. The data indicate that Flag-PECAM-1 binds heparin well at a slightly acidic pH, whereas binding at pH 7.4 is markedly reduced. Binding curves obtained at pH 6.3 and 7.4 are shown for comparison in Figure 2.

To confirm that Flag-PECAM-1 binding to heparin was not an artifact of the expression system, the extracellular domains of PECAM-1 were also expressed as a fusion protein with the Fc and hinge region of human IgG1 fused to domain 6 (PECAM-1-Fc). This protein was expressed in COS-7 cells and purified by affinity chromatography on protein A columns. In solution, these proteins dimerize via the Fc tail. This has the effect of increasing the response units recorded upon SPR analysis, and as expected, PECAM-1-Fc bound well to the heparin-coupled biosensor chip at pH 6.3 (Figure 3A).

Specific Domains of PECAM-1 Are Critical of Heparin Binding. A series of domain deletions of PECAM-1 were constructed and expressed in the Fc-tail expression system. These proteins all contained the N-terminal domain 1, but successive domains from the transmembrane region were deleted to give proteins containing domains 1–5, 1–4, 1–3, 1–2, and 1. These proteins bind to immobilized heparin with varying efficacy depending upon the domains expressed. In particular, domain 1-Fc failed to bind (Figure 3C) and domain 1–2-Fc bound poorly (data not shown), whereas all of the other fusion proteins had binding activity. Binding curves for domain 1–3-Fc are also shown in Figure 3B.

A second set of domain deletions was prepared in the Flag expression system. Because the data indicated that domain 1 did not contain a heparin-binding region, most constructs contained domain 1 to facilitate expression and export from the COS-7 cells. A cartoon of the proteins expressed is given in Figure 4A. The ability of these proteins to bind heparin

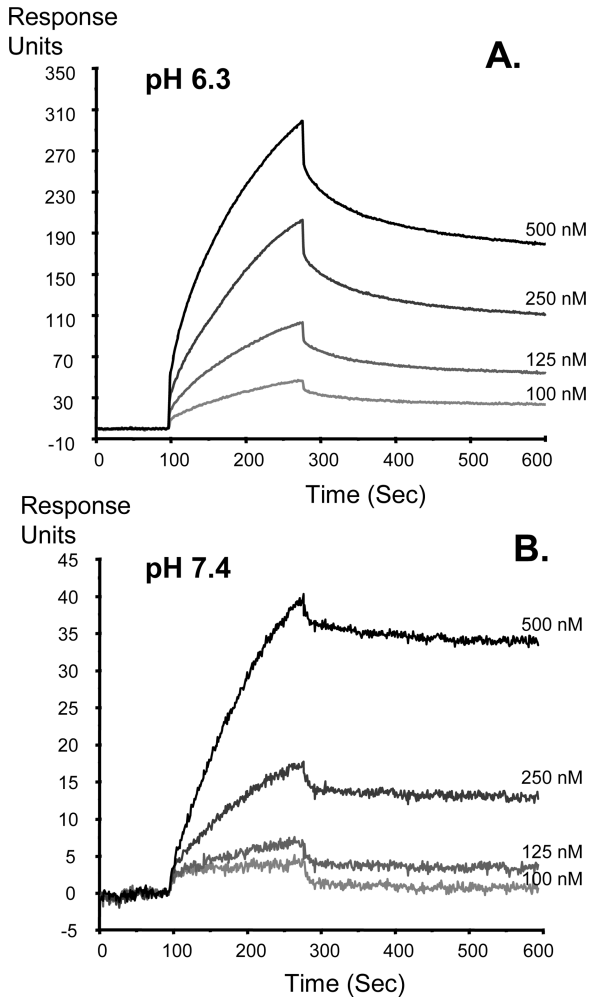

FIGURE 2: PECAM-1 binding to heparin is pH-dependent. Various concentrations of Flag-PECAM-1 in a Bis-Tris saline buffer adjusted to (A) pH 6.3 or (B) pH 7.4 were passed over the heparin-coupled biosensor surface, and sensorgrams were generated.

was examined using an ELISA, where an anti-Flag antibody (M2) was used to immobilize the Flag-PECAM-1 proteins to the wells of ELISA plates and the binding of excess heparin−albumin−biotin (HAB) was determined. These data suggested there are two regions on PECAM-1 that are involved in heparin binding (Figure 4B). HAB binding to Flag-domains 1–3 (D1–3) was comparable to the binding observed when Flag-PECAM-1 (all 6 domains) was immobilized. In contrast, Flag-domains 1–2 was unable to support HAB binding, but Flag-domain 1 fused to domain 3 (D1 plus D3), supporting some binding. These data suggest that one region of heparin binding involves both domains 2 and 3. There appears to be a second heparin-binding site, which involves domains 5 and 6 as Flag-D1 fused to domains 5–6 (D1 plus D5–6) bound HAB, but not to the same extent as Flag-PECAM-1, and Flag-D1 fused to domain 6 (D1 plus D6) did not support binding. Flag-D4–6 also supported HAB binding but less well than Flag-D1 plus D5–6 (Figure 4B).

PECAM-1 Binds Specifically to HS on Melanoma Cell Surfaces. A2058 melanoma cells express high levels of HS on their cell surfaces as revealed by the signal measured by flow cytometry of cells stained with the anti-HS antibody, HepSS-1. HS synthesis can be disrupted by treating cells with chlorate, an inhibitor of ATP sulfurylase and, subsequently, the production of PAPS, the active donor for

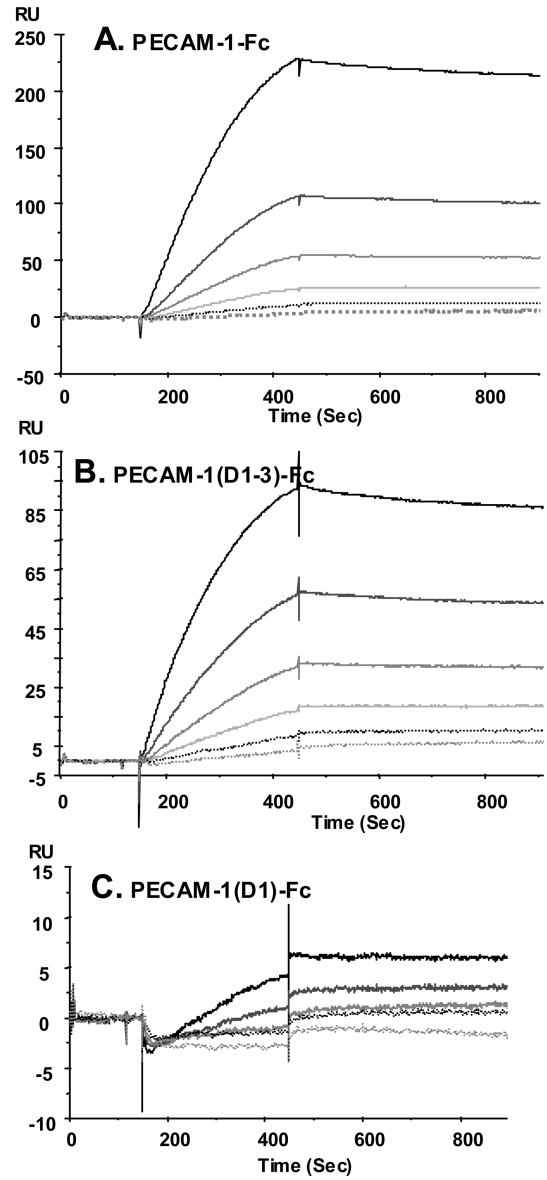

FIGURE 3: PECAM-1-Fc fusion proteins bind heparin differently depending upon the Ig domains expressed. Various Ig domains of PECAM-1 were expressed with the Fc and hinge region of human IgG1 fused to the carboxyl terminus. Proteins were purified and tested for binding to heparin immobilized on a biosensor chip using Bis-Tris saline buffer at pH 6.3. (A) D1–6-Fc, full-length extracellular domains fused to the Fc region; (B) D1–3-Fc, domains 1–3 fused to the Fc region; and (C) D1-Fc, domain 1 fused to the Fc region. The protein concentrations shown are from the top: 250, 125, 62.5, 31.3 (omitted for clarity in C), 15.6, and 7.8 nM.

sulfotransferases. Chlorate treatment decreased reactivity to the HepSS-1 antibody by 81% (data not shown), indicating that cells treated with chlorate do not have correctly sulfated HS on their surfaces. The binding of Flag-PECAM-1 to untreated and chlorate-treated A2058 cells was very different. Flag-PECAM-1 produced a positive signal, well above that of the negative control, when reacted with untreated cells, but after chlorate treatment, the signal resembled that of the negative control (Figure 5A). Heparinase III treatment of melanoma cells similarly caused a very marked decrease in Flag-PECAM-1 binding to these cells (Figure 5B). Mixing Flag-PECAM-1 with HS prior to reacting it with A2058 cells blocked its binding, and the extent of inhibition was dependent upon the concentration of HS used. In contrast,

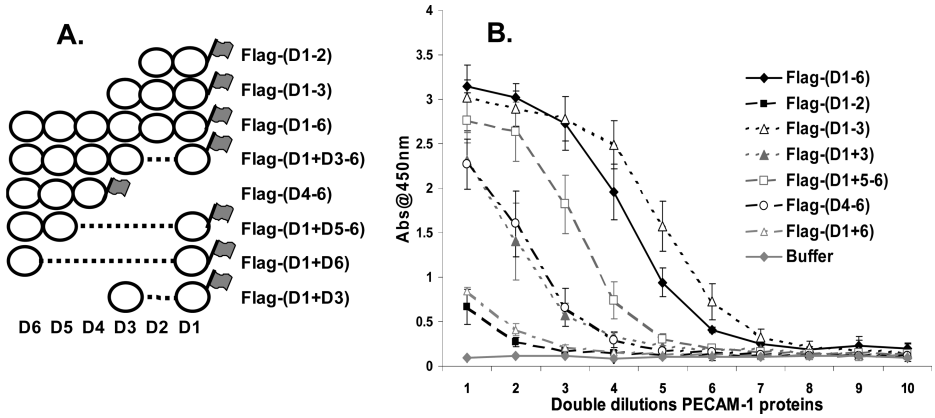

FIGURE 4: Flag-PECAM-1 domains bind heparin differently. (A) Series of domain deletions in which a Flag tag was attached to the N terminus (usually domain 1) that were expressed. (B) Binding to heparin was determined using an ELISA with Bis-Tris saline (pH 6.3) as the binding buffer. Flag-domains were immobilized using the anti-Flag mAb M2. Flag-domains were serially diluted from 80 nM, and HAB was in excess. Biotin was detected using streptavidin−HRP. Mean ± standard errors of three independent experiments are shown.

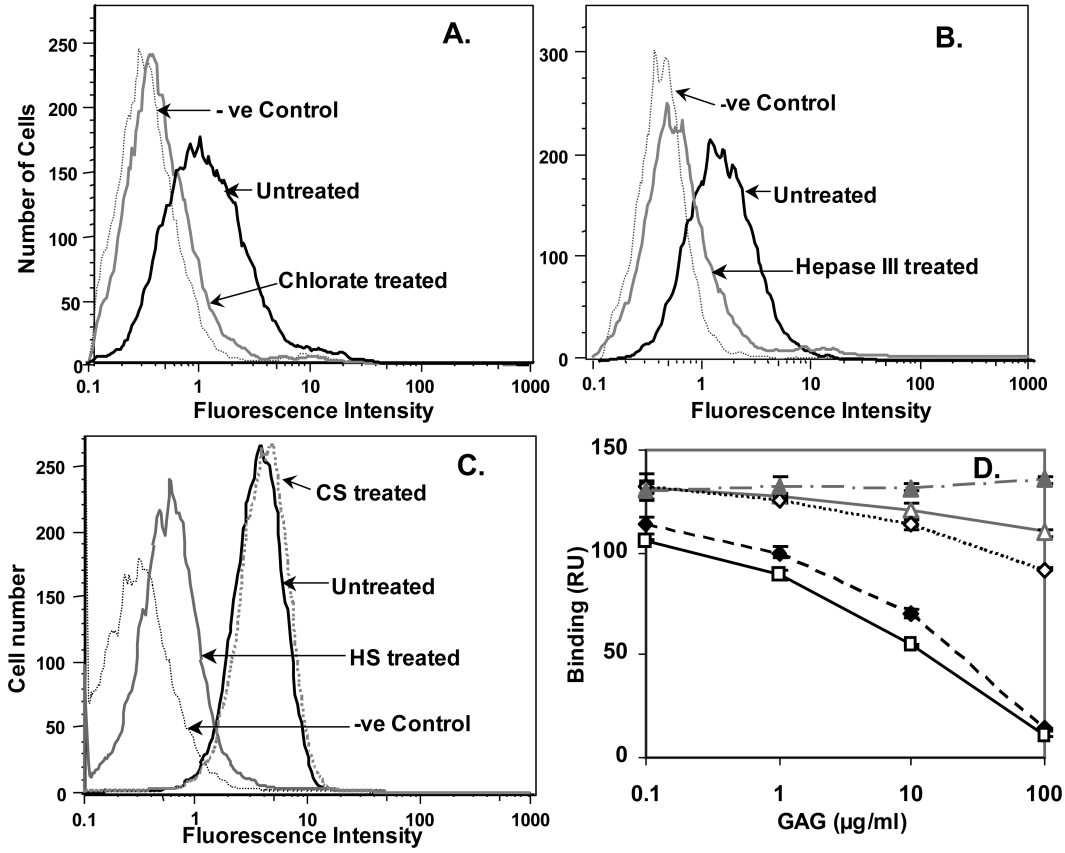

FIGURE 5: Flag-PECAM-1 binds to HS on melanoma cell surfaces. A2058 cells were treated with either (A) chlorate or (B) heparinase III, and binding of Flag-PECAM-1 was visualized using an anti-PECAM-1 polyclonal antibody and FITC-anti-rabbit Ig antibody with detection by flow cytometry. Negative control: no Flag-PECAM-1 but first and second antibodies. Untreated and treated cells are shown. (C) Flag-PECAM-1 mixed with HS (10 μg/test) or chondroitin sulfate C (ChS) (10 μg/test) or without inhibitor was reacted with A2058 cells, and PECAM-1 binding was detected using an anti-sheep polyclonal antibody, anti-sheep Ig-biotin, and streptavidin−Alexa 488. (D) Flag-PECAM-1 (50 nM) was mixed with various GAGs prior to injection over the heparin-coupled biosensor surface. Response units taken at the point when injection ceased are graphed. Means ± standard errors of three replicates are shown. Chondroitin sulfate C (▲), chondroitin sulfate A (△), dermatan sulfate (◇), heparin (◆), and HS (□).

chondroitin sulfate C had little effect on Flag-PECAM-1 binding (Figure 5C).

Flag-D1–3 was seen to bind to A2058 cells in a fashion resembling that of the protein containing the entire extracellular region, Flag-PECAM-1. A clear positive signal, approximately 5 times that of the negative control, was obtained when Flag-D1–3 was reacted with A2058 cells; in contrast, Flag-D1–2 bound very poorly (Figure 6A). The binding of Flag-D1–3 to A2058 cells could be blocked by soluble HS but not by an equal concentration of chondroitin sulfate C (Figure 6B). A similar pattern of specificity was obtained using SPR (Figure 5D). Chondroitin sulfate C did not inhibit binding, even at high concentrations. Chondrotin sulfate A was similar, and chondroitin sulfate B (dermatan sulfate) had slight inhibitory activity at high concentrations. In contrast, both heparin and HS were very effective inhibitors of binding. Collectively, these data indicate that PECAM-1 binds preferentially to heparin/HS-type GAGs.

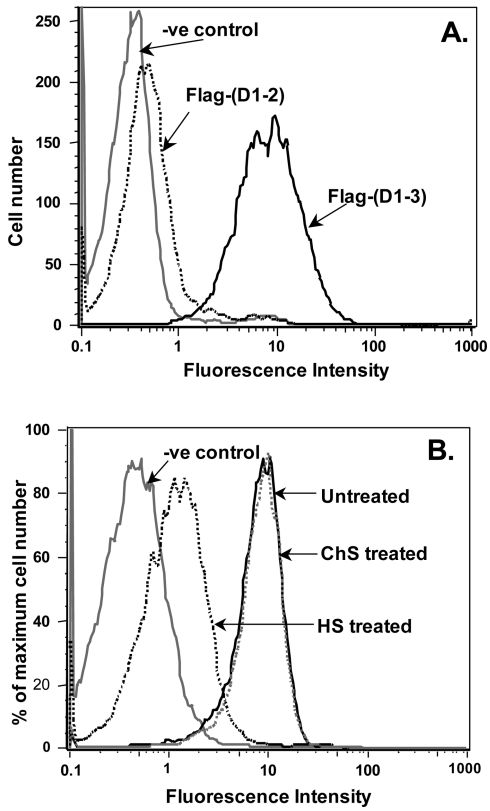

FIGURE 6: Flag-(D1–3) binding to melanoma cell surfaces is blocked by HS. (A) Flag-(D1–3) and Flag-(D1–2), both at 4.2 μg/test were reacted with A2058 cells, and (B) Flag-(D1–3) mixed with HS (50 μg/test) or chondroitin sulfate C (ChS) (50 μg/test) or without inhibitor was reacted with A2058 cells. Binding was visualized using an anti-sheep polyclonal antibody, anti-sheep Ig-biotin, and streptavidin−Alexa 488, with detection by flow cytometry. Negative control: no Flag-proteins but first and second antibodies. Shown are representatives of three separate experiments.

Heparin Fragments DP12 in Length Contain Particular Heparin Structures That Are Recognized by PECAM-1. Heparin fragments were obtained by partial heparinase I digestion of full-length heparin, and separation of the digested products into pools of the same degree of polymerization (DP) was achieved by gel-filtration chromatography. Pools of fragments of size DP4, DP6, DP8, DP10, DP12, DP14, DP16, DP18, and DP20 were obtained. The DP fragment pools were each tested for their ability to inhibit Flag-PECAM-1 binding to heparin immobilized on a biosensor chip. These experiments indicated that the DP12 fragment pool and fragment pools of longer oligosaccharides contain sufficient heparin structures that are recognized by PECAM-1 to inhibit Flag-PECAM-1 from binding (data not shown). The DP12 fragment pool was further fractionated by SAX chromatography to reveal the structural heterogeneity of this pool (Figure 7A). Various subfractions, as indicated in Figure 7A, were collected and tested for their ability to inhibit Flag-PECAM-1−heparin binding in the SPR assay. The best inhibitory activity was seen in subfractions DP12.2 and DP12.8. These subfractions were subjected to a further round of SAX chromatography but were eluted with a shallower salt gradient. This revealed additional structural heterogeneity (Figure 7B), and the fractions indicated in Figure 7B were screened as before for their ability to inhibit Flag-PECAM-1 binding to immobilized heparin. From these data, two of the fractions that had greater activity than their parent subfraction were selected for use in titration experiments. The results of the titration experiments are shown in Figure 7C, and these data indicate that, as the purity of the fractions increases, the inhibitory activity of the fractions also increases. In both cases, lower concentrations of the more pure fractions were required to inhibit binding. Thus, it appears that particular heparin structures are recognized by PECAM-1.

Heparinase III Digestion of HS Produces Fragments That Are Efficiently Recognized by PECAM-1. Because specific structures were recognized by Flag-PECAM-1 from the heparinase I heparin digest, it was argued that possibly a heparinase III digest of HS would produce fragments that contained sulfation motifs recognized by PECAM-1 given that heparinase III cleaves at GlcA residues in unsulfated *N*-acetyl GlcN domains. Indeed, a pool of DP12 HS oligosaccharides prepared by heparinase III digestion was found to inhibit Flag-PECAM-1 from binding to heparin immobilized on a biosensor chip more efficiently than the DP12 pool prepared by heparinase I digestion of heparin. Sensorgrams comparing Flag-PECAM-1 binding in the presence of the HS DP12 pool indicated that on a molar basis this material inhibits as effectively the parent HS (Figure 8). Moreover, preliminary data are suggesting that a DP8 pool of this material is similarly effective (data not shown).

Modeling of the Binding of Heparin Fragments to Domains 2 and 3 of PECAM-1. The preceding paper (*27*) describes docking simulations of various GAG fragments to the extracellular domains of PECAM-1. This work has indicated that a heparin pentasaccharide binds most strongly to a region that involves domains 2 and 3. Because particular heparin/HS fragments were more effective than others at blocking PECAM-1 from binding to immobilized heparin, further modeling of the interactions with domains 2 and 3 of a number of DP5 and DP6 structures containing iduronic acid residues in different conformations was performed. Docking of oligosaccharides smaller than a pentasaccharide suggested that these bound poorly to this region (data not shown). Of the two pentasaccharides docked [extracted from PDB structures 1QQP (*30*) and 2HYV (*31*)], the one from 2HYV, in which the iduronic acid, residue A, is in the $^1H_2$ conformation and iduronic acids C and D are in the $^1C_4$ conformation, had the lowest free energy of binding (Table 2). The pentasaccharide from 1QQP differs from that of 2HYV in that the IdoA2S in position C is in the $^2S_0$ conformation, which leads to a different glycosidic torsion angle, and consequently, this fragment lacks the significant interactions between GlcNS6S in position B and the protein surface seen with the pentasaccharide of 2HYV [see preceding paper (*27*)].

Modeling of the hexasaccharides also suggested that structural features of the uronic acids were important for binding. A hexasaccharide extracted from PDB structure 1BFC (*32*), having a ΔUA2S as residue A in the $^1H_2$ conformation and an IdoA2S in a $^2S_0$ conformation as residue E, failed to bind because none of the docked binding poses showed a good fit between the sulfates and the basic amino acids identified as the GAG-binding site in domains 2 and 3. The hydroxyl of the GlcNS6S, residue B, made a hydrogen bond with the side chain of Lys 255, and the 6-*O*-sulfate made electrostatic interactions with His 239; however, most of the 2-*O*-sulfate groups on the IdoA2S residues protruded away from the protein surface. Docking results using the

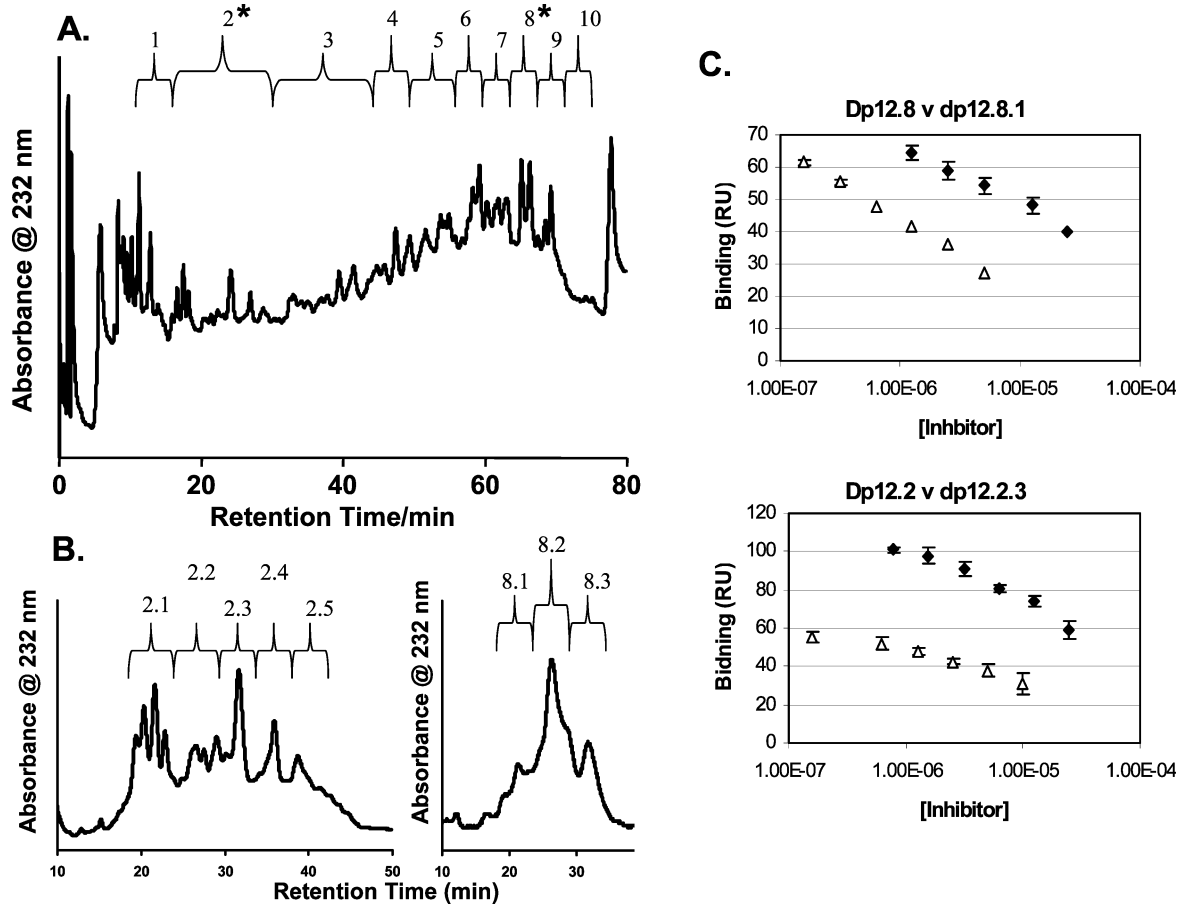

FIGURE 7: Certain DP12 heparin fragments preferentially bind PECAM-1. (A) DP12 pool of fragments generated by heparinase I digestion of heparin was fractionated by SAX on PA1 columns. The subfractions collected are indicated. (B) Subfractions 2 and 8 (DP12.2 and DP12.8) were subjected to further SAX-HPLC and indicated sub-subfractions collected. (C) Ability of these sub-subfractions to inhibit Flag-PECAM-1 from binding immobilized heparin was compared to that of parent subfractions. Shown are the most active parent subfractions, either DP12.8 or DP12.2 (◆) and sub-subfractions either DP12.8.1 or DP12.2.3 (△). Response units taken at the point when injection ceased are graphed. Means ± standard errors of three replicates are shown.

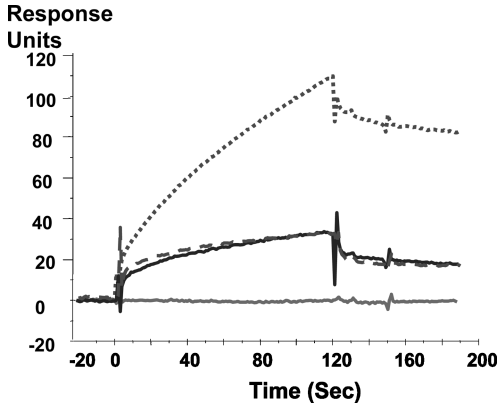

FIGURE 8: DP12 fractions prepared by heparinase III cleavage of HS are as effective as full-length HS in blocking Flag-PECAM-1 from binding to heparin coupled to a biosensor flow cell surface. Flag-PECAM-1 (1 μM) in Bis-Tris saline buffer at pH 6.3 was mixed with either DP12 HS fragments (2.5 μM) or full-length HS (2.5 μM) prior to injection. Sensorgrams of Flag-PECAM-1 (dotted line), Flag-PECAM-1 plus DP12 HS (gray dashed line), Flag-PECAM-1 plus full-length HS (black solid line), and negative control of Flag-PECAM-1 interacting with a control flow cell surface (solid gray line) are shown.

hexasaccharide structure from 1XT3 (*33*) indicated that it had fewer electrostatic interactions and hydrogen bonds than the pentasaccharide from 2HYV (*31*). This is reflected in the predicted small free energy of binding of the top-ranking binding pose (Table 2). In the hexasaccharide from 1XT3, the IdoA2S in residue E is in the $^2S_0$ skew-boat conformation. Construct 1 was a hexasaccharide made to include the tetrasaccharide B−E from 2HYV. The docking of construct 1 was performed with restrained interglycosidic torsions but flexible substituents. The free energy of binding was corrected to account for the missing rotational entropy with respect to the docking of saccharides with full conformational freedom. The predicted binding mode of construct 1 was similar to that of the pentasaccharide fragment from which it was constructed, with a root-mean-square deviation (rmsd) of 0.759 Å. Interestingly, the systematic docking procedure did not identify an energetically favored binding mode upon flexible docking, although there is no steric hindrance to construct 1 interacting with domains 2 and 3. Docking calculations performed using both methods identified the same binding mode but produced different internal energies of interaction. Despite its greater length, construct 1 makes the same interactions with domains 2 and 3 through its last five residues (A–E) as the parent structure from 2HYV [see preceding paper (*27*)], with the *N*-sulfate of residue A′ establishing an electrostatic interaction with the protonated $N_{\varepsilon 2}$ in His 253 (Figure 9). However, the 6-*O*-sulfate on saccharide A′ points away from the protein surface and hence does not produce any increase in binding affinity.

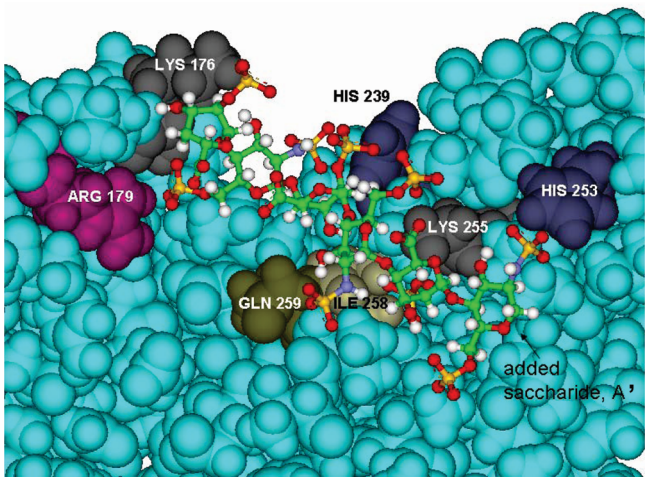

FIGURE 9: Predicted binding mode of the heparin hexasaccharide (construct 1) to Ig domains 2 and 3 of PECAM-1. The interactions between the hexasaccharide fragment and the protein are similar to those predicted to be important for the binding of the pentasaccharide fragment extracted from 2HYV, with the additional saccharide, A′, interacting with His 253. Amino acids involved in the interaction are highlighted.

DISCUSSION

The aim of this study was to revisit whether PECAM-1 is able to bind GAGs of the heparin/HS family in a way that has physiological relevance. Here, we have used two quite different protein expression systems to produce the extracellular domains of PECAM-1, and the data obtained for heparin/HS binding are comparable for both types of PECAM-1 proteins. Our data clearly demonstrates that PECAM-1 can bind to heparin and HS in biochemical experiments and to HS on cell surfaces. Binding occurs optimally at a pH that is slightly acidic, as is the case for a number of other proteins that bind heparin/HS by a site that includes one or more histidines (*29*). The data suggest that PECAM-1 recognizes heparin/HS structures that have a particular pattern of sulfation, and molecular modeling studies highlight the importance of the conformation of IdoA residues in the GAG structure that binds.

PECAM-1 joins a growing number of proteins that bind heparin/HS under slightly acidic conditions, including avidin, granulocyte-macrophage colony-stimulating factor (GM-CSF), mast-cell tryptase, clusterin, histidine−proline-rich glycoprotein, the nonfribrillar form of β-amyloid peptide, and vascular endothelial growth factor (VEGF) (*22, 34–39*). It is well-known that at sites of tissue damage or inflammation the local pH can drop well below neutral. This is attributed to a local increase in lactic acid production, which is caused by the anaerobic glycolysis of infiltrating neutrophils. The pH of fluids drained from inflammatory sites indicates an extracellular pH as low as 6.1 (*40*). Hypoxia or ischemia is also associated with local acidosis. The preferential binding of proteins to HS under acidic conditions may have a regulatory role. The pH-dependent binding of VEGF to HS in the extracellular matrix is believed to facilitate the establishment of a VEGF gradient to direct and stimulate the growth of new blood vessels into hypoxic or ischemic regions in tissues (*41*).

It is likely that the pH dependency of the interaction of PECAM-1 with HS also serves to regulate the function of the protein. It has been demonstrated that a deficiency in endothelial HS impairs neutrophil trafficking in response to inflammation (*42*). Similarly, the loss of the basement membrane HS proteoglycan perlecan impairs early monocyte/macrophage influx following renal ischemia and subsequent reperfusion (*43*). Ischemia/reperfusion damages the endothelium, thereby exposing the microvascular basement membrane. Although in both cases the contribution of HS was explained in terms of its role as a chemokine and L-selectin ligand, it is probable that the binding of HS to PECAM-1 on leukocytes also acts to regulate cellular infiltration of inflamed sites. Tumor microenvironments are commonly acidic, with pH values as low as 5.5 being recorded. The demonstration that PECAM-1 can bind to HS on melanoma cell surfaces suggests that endothelial PECAM-1 could contribute to melanoma cell intra- and extravasation during metastasis.

The literature on the possible interaction of PECAM-1 with heparin/HS has been confused. The early studies supported such an interaction (*14, 15*), citing the motif in Ig domain 2, LKREKN, which loosely resembles a GAG-binding consensus sequence as proposed by Cardin and Weintraub (*44*). A number of papers suggesting that the cytoplasmic tail controls whether PECAM-1 engages in homo- or heterophilic binding events followed. In these studies, deletions in exon 14 or alternative splicing events, which eliminated exon 14, were seen to direct PECAM-1 to heparin-independent homophilic adhesion as determined by aggregation assays of transfected and nontransfected L cells (*20, 21, 45*). A further study examined the adhesive properties of multivalent (PECAM-1/Ig chimeric proteins and PECAM-1 proteoliposomes) and monovalent PECAM-1, and no evidence for GAG binding was obtained. It was concluded that GAGs indirectly affect PECAM-1-mediated cell−cell adhesion by inhibition of events downstream of PECAM-1-binding events (*18*).

The present study clarifies the confusion. PECAM-1 does bind GAGs of the heparin/HS family, but this binding is pH-sensitive. Both the dimeric PECAM-1-Fc fusion protein and Flag-PECAM-1 bound heparin in SPR assays and HS on cell surfaces at a pH below 6.5. Our PECAM-1-Fc fusion proteins do not contain the basic hinge region deemed necessary for heparin binding by Sun et al. (*18*). Moreover, the Flag-tagged proteins terminate at the end of domain 6. Thus, the heparin/HS binding described in this study is not an artifact of the protein-expression systems used. The domain deletion studies using both expression systems have identified the prime GAG-binding site as requiring both domains 2 and 3. The binding data indicate that domain 2 on its own is not sufficient for stable PECAM-1-heparin binding, but when domain 2 and domain 3 are expressed together, binding occurs. This conclusion is supported by the modeling study described in the preceding paper (*27*). The modeling suggests that the heparin-binding site involves residues in and around the Cardin and Weintraub GAG-binding consensus motif in domain 2, particularly, K176, L177, and R179, but also the basic residues H239, K255, and H253 of domain 3 (numbering system from Swiss-Prot P16284). The involvement of two histidines in the GAG-binding site detected by molecular modeling is in direct agreement with the biochemical evidence regarding the pH dependency of heparin binding. Data described in this present

study and the modeling study also support a second, less important heparin-binding region that involves domains 5 and 6, but more work needs to be performed to verify this. Interestingly, both GAG-binding regions are distinct from sites described as involved in PECAM-1 homophilic binding (*11*).

Heparin and HS are mixtures of linear chains that are extremely structurally diverse. The chains differ in length, in monosaccharide sequence, and in patterns of sulfation. GAGs of this family are composed of repeating disaccharide units consisting of a hexuronic acid linked to a glucosamine; the uronic acid is either a β-D-glucuronic acid (GlcA) or an α-L-iduronic acid (IdoA). All of these components can occur as unmodified saccharides, or they may be sulfated at various positions. It is the three-dimensional structure of the heparin or HS chain and the pattern of the negative charge that is presented that determines whether a particular heparin/HS fragment will bind a protein (*29*). Some proteins bind very particular motifs within heparin/HS chains, whereas others are more promiscuous. The possibility that PECAM-1 may bind to particular heparin/HS structures was explored.

Heparin fragments were produced by cleaving with heparinase I. This enzyme cleaves at highly sulfated regions of the GAG chain; therefore, the fragments are likely to have highly sulfated termini, but internal saccharides may not be fully sulfated. The screening analysis revealed that, within a pool of DP12 fragments, a small subpopulation of fragments bound better to PECAM-1 than others and, as these fragments were purified, the apparent activity of these structures increased with purification. The fragments produced by heparinase III cleavage of HS should have a structure whereby the internal saccharides are highly sulfated (possibly consisting of repeats of the trisulfated disaccharide), while the terminal saccharides carry less sulfates. It appears that the HS fragments contain a greater PECAM-1-binding activity within smaller fragments than that observed with the heparin fragments. In particular, DP12 HS fragments were as effective as full-length HS at blocking binding to immobilized heparin, and preliminary experiments with DP8 fragments are indicating similar levels of activity for these fragments. The need for a highly sulfated motif is supported by the modeling studies. Collectively, these data suggest that the PECAM-1-binding motif is highly sulfated, that certain sulfation patterns are preferred for binding, and that the natural binding motif is DP8 or smaller. Other heparin/HS-binding proteins have also demonstrated a preference for certain sulfation patterns while binding others with lower affinities; for example, FGF-1 binds a number of structures but with graded affinities (*46*). It is likely that the affinity of PECAM-1 interactions with various heparin/HS structures will also be graded.

Interestingly, chondroitin sulfates A and C failed to show evidence of PECAM-1 reactivity in the SPR assay and the melanoma cell binding assay. This pattern of reactivity is consistent with that seen in our earlier study (*15*) and with the modeling described in the preceding paper (*27*). It appears that chondroitin sulfate B (dermatan sulfate) fragments may bind but markedly less well than heparinoid fragments. This points to the importance of IdoA residues in the saccharide structure, probably because of their flexibility.

In solution, the IdoA residues of heparin and HS oscillate between the $^1C_4$ and the $^2S_0$ conformations and the equilibrium between these conformations is very rapid, indicating a very low energy barrier between the two forms. The equilibrium between these two IdoA forms lies toward the $^1C_4$ when it occurs as an internal residue in a heparinoid chain (*47*). Nevertheless, it may be expected that, when interacting with a protein, the protein will cause this equilibrium to be perturbed and therefore select the conformation that is most energetically favored for a stable interaction. Experimental evidence for this conclusion exists for antithrombin III and FGF-2 interactions with heparin structures (*29*). The modeling method used here does not allow for any oscillation between the two IdoA forms, but we have modeled structures where the IdoA residues have been fixed in different conformations. These studies suggest that uronic acid isomers of IdoA in the $^1C_4$ chair configuration favor binding to domains 2 and 3 of PECAM-1.

The modeling also suggests that structures as small as a pentasaccharide can bind to domains 2 and 3, but no experimental evidence of this has been obtained. The comparison between the pentasaccharide from 2HYV and the hexasaccharide, construct 1, which includes the tetrasaccharide from the 2HYV structure, suggests that key interactions occur between six sulfates in the 2HYV structure, and although saccharide A′ of construct 1 established an additional electrostatic interaction with His 253, no increase in binding affinity was recorded. Clearly, the free energies calculated from such a modeling study are an approximation of the natural situation and are dependent upon the configuration of the PECAM-1 domains that have been constructed in the model. These calculations assumed a closed configuration of domains 2 and 3 (*27*); it is likely that in nature these two domains may not always be in such close proximity.

This study clearly demonstrates that PECAM-1 does bind heparin/HS structures under conditions of mild acidosis that occur at sites of inflammation and in tumor microenvironments or following prolonged ischemia. Further studies are required to determine whether motifs more selective than the repeating trisulfated disaccharides that were modeled are recognized by PECAM-1 and whether these motifs are located on specific cells or tissues. Nevertheless, it is likely that the binding of PECAM-1 to HS *in vivo* is controlled by both the local pH and the particular HS structures that bind most favorably. Because the GAG-binding sites are distinct and removed from those regions required for PECAM-1 homophilic interactions, it is possible that *in vivo* the two types of binding, HS-PECAM-1 heterophilic binding and PECAM-1 homophilic binding, could occur at tissue locations and under disease conditions, where local acidosis is prevalent. Indeed, leukocyte infiltration of inflamed tissues is likely to be regulated by both types of PECAM-1-binding events. A review of the functions of PECAM-1 in the light of these findings is desirable.

ACKNOWLEDGMENT

We gratefully acknowledge the Western Australian Interactive Virtual Environments Centre (IVEC) for access to high-performance computing facilities.

REFERENCES

1. Newman, P. J. (1997) The biology of PECAM-1. *J. Clin. Invest. 99*, 3–8.

2. Newton, J. P., Hunter, A. P., Simmons, D. L., Buckley, C. D., and Harvey, D. J. (1999) CD31 (PECAM-1) exists as a dimer and is heavily N-glycosylated. *Biochem. Biophys. Res. Commun. 261*, 283–291.
3. Wang, Y., Su, X., Sorenson, C. M., and Sheibani, N. (2003) Tissue-specific distributions of alternatively spliced human PECAM-1 isoforms. *Am. J. Physiol. Heart Circ. Physiol. 284*, H1008–H1017.
4. O'Brien, C. D., Cao, G., Makrigiannakis, A., and DeLisser, H. M. (2004) Role of immunoreceptor tyrosine-based inhibitory motifs of PECAM-1 in PECAM-1-dependent cell migration. *Am. J. Physiol. Cell Physiol. 287*, C1103–C1113. .
5. Schenkel, A. R., Chew, T. W., and Muller, W. A. (2004) Platelet endothelial cell adhesion molecule deficiency or blockade significantly reduces leukocyte emigration in a majority of mouse strains. *J. Immunol. 173*, 6403–6408.
6. Zocchi, M. R., and Poggi, A. (2004) PECAM-1, apoptosis and CD34+ precursors. *Leuk. Lymphoma 45*, 2205–2213.
7. Gibbins, J. M. (2004) Platelet adhesion signalling and the regulation of thrombus formation. *J. Cell Sci. 117*, 3415–3425.
8. Dhanjal, T. S., Ross, E. A., Auger, J. M., McCarty, O. J., Hughes, C. E., Senis, Y. A., Buckley, C. D., and Watson, S. P. (2007) Minimal regulation of platelet activity by PECAM-1. *Platelets 18*, 56–67.
9. Dhanjal, T. S., Pendaries, C., Ross, E. A., Larson, M. K., Protty, M. B., Buckley, C. D., and Watson, S. P. (2007) A novel role for PECAM-1 in megakaryocytokinesis and recovery of platelet counts in thrombocytopenic mice. *Blood 109*, 4237–4244.
10. Wang, L., Menendez, P., Cerdan, C., and Bhatia, M. (2005) Hematopoietic development from human embryonic stem cell lines. *Exp. Hematol. 33*, 987–996.
11. Newton, J. P., Buckley, C. D., Jones, E. Y., and Simmons, D. L. (1997) Residues on both faces of the first immunoglobulin fold contribute to homophilic binding sites of PECAM-1/CD31. *J. Biol. Chem. 272*, 20555–20563.
12. Buckley, C. D., Doyonnas, R., Newton, J. P., Blystone, S. D., Brown, E. J., Watt, S. M., and Simmons, D. L. (1996) Identification of $\alpha_v\beta_3$ as a heterotypic ligand for CD31/PECAM-1. *J. Cell Sci. 109* (2), 437–445.
13. Deaglio, S., Morra, M., Mallone, R., Ausiello, C. M., Prager, E., Garbarino, G., Dianzani, U., Stockinger, H., and Malavasi, F. (1998) Human CD38 (ADP-ribosyl cyclase) is a counter-receptor of CD31, an Ig superfamily member. *J. Immunol. 160*, 395–402.
14. DeLisser, H. M., Yan, H. C., Newman, P. J., Muller, W. A., Buck, C. A., and Albelda, S. M. (1993) Platelet/endothelial cell adhesion molecule-1 (CD31)-mediated cellular aggregation involves cell surface glycosaminoglycans. *J. Biol. Chem. 268*, 16037–16046.
15. Watt, S. M., Williamson, J., Genevier, H., Fawcett, J., Simmons, D. L., Hatzfeld, A., Nesbitt, S. A., and Coombe, D. R. (1993) The heparin binding PECAM-1 adhesion molecule is expressed by CD34+ hematopoietic precursor cells with early myeloid and B-lymphoid cell phenotypes. *Blood 82*, 2649–2663.
16. Sachs, U. J., Andrei-Selmer, C. L., Maniar, A., Weiss, T., Paddock, C., Orlova, V. V., Choi, E. Y., Newman, P. J., Preissner, K. T., Chavakis, T., and Santoso, S. (2007) The neutrophil-specific antigen CD177 is a counter-receptor for platelet endothelial cell adhesion molecule-1 (CD31). *J. Biol. Chem. 282*, 23603–23612.
17. Wong, C. W., Wiedle, G., Ballestrem, C., Wehrle-Haller, B., Etteldorf, S., Bruckner, M., Engelhardt, B., Gisler, R. H., and Imhof, B. A. (2000) PECAM-1/CD31 trans-homophilic binding at the intercellular junctions is independent of its cytoplasmic domain; evidence for heterophilic interaction with integrin $\alpha_v\beta_3$ in cis. *Mol. Biol. Cell 11*, 3109–3121.
18. Sun, Q. H., Paddock, C., Visentin, G. P., Zukowski, M. M., Muller, W. A., and Newman, P. J. (1998) Cell surface glycosaminoglycans do not serve as ligands for PECAM-1. PECAM-1 is not a heparin-binding protein. *J. Biol. Chem. 273*, 11483–11490.
19. Muller, W. A., Berman, M. E., Newman, P. J., DeLisser, H. M., and Albelda, S. M. (1992) A heterophilic adhesion mechanism for platelet/endothelial cell adhesion molecule 1 (CD31). *J. Exp. Med. 175*, 1401–1404.
20. Yan, H. C., Baldwin, H. S., Sun, J., Buck, C. A., Albelda, S. M., and DeLisser, H. M. (1995) Alternative splicing of a specific cytoplasmic exon alters the binding characteristics of murine platelet/endothelial cell adhesion molecule-1 (PECAM-1). *J. Biol. Chem. 270*, 23672–23680.
21. Famiglietti, J., Sun, J., DeLisser, H. M., and Albelda, S. M. (1997) Tyrosine residue in exon 14 of the cytoplasmic domain of platelet endothelial cell adhesion molecule-1 (PECAM-1/CD31) regulates ligand binding specificity. *J. Cell Biol. 138*, 1425–1435.
22. Kett, W. C., Osmond, R. I., Moe, L., Skett, S. E., Kinnear, B. F., and Coombe, D. R. (2003) Avidin is a heparin-binding protein. Affinity, specificity and structural analysis. *Biochim. Biophys. Acta 1620*, 225–234.
23. Fawcett, J., Buckley, C., Holness, C. L., Bird, I. N., Spragg, J. H., Saunders, J., Harris, A., and Simmons, D. L. (1995) Mapping the homotypic binding sites in CD31 and the role of CD31 adhesion in the formation of interendothelial cell contacts. *J. Cell Biol. 128*, 1229–1241.
24. Osmond, R. I., Kett, W. C., Skett, S. E., and Coombe, D. R. (2002) Protein−heparin interactions measured by BIAcore 2000 are affected by the method of heparin immobilization. *Anal. Biochem. 310*, 199–207.
25. Chai, W., Luo, J., Lim, C. K, and Lawson, A. M. (1998) Characterization of heparin oligosaccharide mixtures as ammonium salts using electrospray mass spectrometry. *Anal. Chem. 70*, 2060–2066.
26. Kett, W. C., and Coombe, D. R. (2004) A structural analysis of heparin-like glycosaminoglycans using MALDI−TOF mass spectrometry. *Spectroscopy 18*, 185–201.
27. Gandhi, N. S., Coombe, D. R., and Mancera, R. L. Platelet endothelial cell adhesion molecule 1 (PECAM-1) and its interactions with glycosaminoglycans: 1. Molecular modeling studies, *Biochemistry* 2008, in press.
28. Morris, G. M., Goodsell, D. S., Halliday, R. S., Huey, R., Hart, W. E., Belew, R. K., and Olson, A. J. (1998) Automated docking using a Lamarckian genetic algorithm and an empirical binding free energy function. *J. Comput. Chem. 19*, 1639–1662.
29. Coombe, D. R., and Kett, W. C. (2005) Heparan sulfate−protein interactions: Therapeutic potential through structure−function insights. *Cell. Mol. Life Sci. 62*, 410–424.
30. Fry, E. E., Lea, S. M., Jackson, T., Newman, J. W., Ellard, F. M., Blakemore, W. E., Abu-Ghazaleh, R., Samuel, A., King, A. M., and Stuart, D. I. (1999) The structure and function of a foot-and-mouth disease virus−oligosaccharide receptor complex. *EMBO J. 18*, 543–554.
31. Shao, C., Zhang, F., Kemp, M. M., Linhardt, R. J., Waisman, D. M., Head, J. F., and Seaton, B. A. (2006) Crystallographic analysis of calcium-dependent heparin binding to annexin A2. *J. Biol. Chem. 281*, 31689–31695.
32. Faham, S., Hileman, R. E., Fromm, J. R., Linhardt, R. J., and Rees, D. C. (1996) Heparin structure and interactions with basic fibroblast growth factor. *Science 271*, 1116–1120.
33. Lee, S. C., Guan, H. H., Wang, C. H., Huang, W. N., Tjong, S. C., Chen, C. J., and Wu, W. G. (2005) Structural basis of citrate-dependent and heparan sulfate-mediated cell surface retention of cobra cardiotoxin A3. *J. Biol. Chem. 280*, 9567–9577.
34. Wettreich, A., Sebollela, A., Carvalho, M. A., Azevedo, S. P., Borojevic, R., Ferreira, S. T., and Coelho-Sampaio, T. (1999) Acidic pH modulates the interaction between human granulocyte-macrophage colony-stimulating factor and glycosaminoglycans. *J. Biol. Chem. 274*, 31468–31475.
35. Hallgren, J., Backstrom, S., Estrada, S., Thuveson, M., and Pejler, G. (2004) Histidines are critical for heparin-dependent activation of mast cell tryptase. *J. Immunol. 173*, 1868–1875.
36. Pankhurst, G. J., Bennett, C. A., and Easterbrook-Smith, S. B. (1998) Characterization of the heparin-binding properties of human clusterin. *Biochemistry 37*, 4823–4830.
37. Borza, D. B., and Morgan, W. T. (1998) Histidine−proline-rich glycoprotein as a plasma pH sensor. Modulation of its interaction with glycosaminoglycans by pH and metals. *J. Biol. Chem. 273*, 5493–5499.
38. Gupta-Bansal, R., Frederickson, R. C., and Brunden, K. R. (1995) Proteoglycan-mediated inhibition of A^{β} proteolysis. A potential cause of senile plaque accumulation. *J. Biol. Chem. 270*, 18666–18671.
39. Goerges, A. L., and Nugent, M. A. (2003) Regulation of vascular endothelial growth factor binding and activity by extracellular pH. *J. Biol. Chem. 278*, 19518–19525.
40. Trevani, A. S., Andonegui, G., Giordano, M., Lopez, D. H., Gamberale, R., Minucci, F., and Geffner, J. R. (1999) Extracellular acidification induces human neutrophil activation. *J. Immunol. 162*, 4849–4857.
41. Goerges, A. L., and Nugent, M. A. (2004) pH regulates vascular endothelial growth factor binding to fibronectin: A mechanism for control of extracellular matrix storage and release. *J. Biol. Chem. 279*, 2307–2315.
42. Wang, L., Fuster, M., Sriramarao, P., and Esko, J. D. (2005) Endothelial heparan sulfate deficiency impairs L-selectin- and

chemokine-mediated neutrophil trafficking during inflammatory responses. *Nat. Immunol. 6*, 902–910.

43. Celie, J. W., Rutjes, N. W., Keuning, E. D., Soininen, R., Heljasvaara, R., Pihlajaniemi, T., Drager, A. M., Zweegman, S., Kessler, F. L., Beelen, R. H., Florquin, S., Aten, J., and van den Born, J. (2007) Subendothelial heparan sulfate proteoglycans become major L-selectin and monocyte chemoattractant protein-1 ligands upon renal ischemia/reperfusion. *Am. J. Pathol. 170*, 1865–1878.
44. Cardin, A. D., and Weintraub, H. J. (1989) Molecular modeling of protein−glycosaminoglycan interactions. *Arteriosclerosis 9*, 21–32.
45. DeLisser, H. M., Chilkotowsky, J., Yan, H. C., Daise, M. L., Buck, C. A., and Albelda, S. M. (1994) Deletions in the cytoplasmic domain of platelet endothelial cell adhesion molecule-1 (PECAM-1, CD31) result in changes in ligand binding properties. *J. Cell Biol. 124*, 195–203.
46. Kreuger, J., Salmivirta, M., Sturiale, L., Gimenez-Gallego, G., and Lindahl, U. (2001) Sequence analysis of heparan sulfate epitopes with graded affinities for fibroblast growth factors 1 and 2. *J. Biol. Chem. 276*, 30744–30752.
47. Conrad, H. E. (1998) *Heparin-Binding Proteins*, Academic Press, San Diego, CA.

BI7024595